A Miniaturization Band-Pass Filter with Ultra-Narrow Multi-Notch-Band Characteristic for Ultra-Wideband Communication Applications

Yingsong Li [1], Wenxing Li [1], Wenhua Yu [1,2], and Chengyuan Liu [1]

[1] College of Information and Communications Engineering
Harbin Engineering University, Harbin 150001, China
liyingsong82@gmail.com, liwenxing@hrbeu.edu.cn, liuchengyuan@hrbeu.edu.cn

[2] 2COMU, Inc.
4031 University Drive, Suite 100, Fairfax, VA 22030, USA
wenyu@2comu.com

Abstract ─ In this paper, we present a novel approach for designing compact Ultra-Wideband (UWB) band-pass filters with desired multi-notch-band characteristics. The multi-notch-band features are realized by using a ring-stub multi-mode resonator, while the equivalent model is also obtained by using the odd/even excitation resonance condition. The fabricated prototype of the band-pass multi-notch-band filter demonstrates a good behavior as expected. Simulated and experimental results show that the proposed filter with a compact size of 25×10 mm^2, has an impedance bandwidth between 3.0 GHz and 10.6 GHz; while the multiple notch bands are achieved and their center frequencies are located at 3.9 GHz, 5.25 GHz, 5.9 GHz, 6.8 GHz and 8.0 GHz. The proposed filter is suitable for being integrated in UWB radio systems to efficiently enhance the interference immunity from unexpected signals, such as Worldwide Interoperability for Microwave Access (WiMAX), Wireless Local-Area Network (WLAN), 6.8 GHz Radio Rrequency Identification (RFID) communication and X-band satellite communications.

Index Terms - Band-pass filter, multi-notch band characteristics, notch band filter and UWB filter.

I. INTRODUCTION

Since the Federal Communications Commission (FCC) released the frequency band from 3.1 GHz to 10.6 GHz for commercial communication applications in February 2002, the Ultra-Wideband (UWB) radio system has been receiving more attention in both academic and industrial fields [1]. An UWB Band-Pass Filter (BPF) is one of the key passive components to realize an UWB radio system; which has attracted more attention recently. A great number of methods have been proposed in order to design BPFs with large Fractional Bandwidths (FBW) and good performance [2-6]. There have existed the typical structures, including low and high-pass filter configurations [2], Coplanar Waveguide (CPW) geometries [3], right/left-handed structures [4], microstrip cascaded fork-form resonator [5] and defected ground structure [6]. However, there are some drawbacks in these designs, such as out-of-band performance and complicated structure.

On the other hand, there are some existing narrow-band systems which have been used in the communications for a long time. Furthermore, the UWB frequency band overlaps with these existing narrow communication systems, such as WiMAX in 3.4 GHz to 3.69 GHz band, WLAN in 5.2 GHz and 5.8 GHz bands and 6.8 GHz RFID band. Those narrowband radio signals might interfere with UWB systems and vice versa. To mitigate the potential interference, design of compact UWB BPFs with notched band characteristics is one of the most challenging topics. Consequently, a number of methods have been proposed and investigated to design UWB BPFs with notched bands [7-22], such as embedded Complementary Split Ring Resonators (CSRR) [7], Defected

Submitted On: April 27, 2013
Accepted On: April 19, 2014

Ground Structures (DGS) [8,11], mismatch transmission lines [9], short-circuited stubs [10]; which can effectively reject unexpected radio signals. Nevertheless, some of these previously proposed band-notched UWB filters are still large in size [7], incompatible with Monolithic Microwave Integrated Circuits (MMIC) [8], complicated in structures [9] and sophisticated in band rejection characteristic design [7-11].

In this paper, we present a novel approach to designing compact Ultra-Wideband (UWB) band-pass filter with a good multi-notch-band characteristic. The proposed multi-notch-band characteristic is realized by using Ring-Stub Multi-Mode Resonator (RSMMR). The resonance condition of RSMMR is obtained by means of odd and even mode theorem [14]. In comparison with the existing UWB notch-band filter in [7-13], the proposed notched bands can be easily operated simultaneously. Performance of the proposed filter is validated by fabricating the proposed multi-notch-band band-pass UWB filter on a RT/Duorid 6006 substrate, that has a relative dielectric constant of 6.15 and a thickness of 0.635 mm.

II. FILTER DESIGN

In this section, the design procedure and synthesis method of the proposed compact UWB BPF with multi-notch bands are described on the basis of loading stub technique. Generally speaking, the proposed filter essentially exploits Multi-Mode Resonator (MMR) structures to realize the sharp and adjustable multi-notch-band.

The schematic diagram of the proposed UWB BPF with multi-notch-band characteristics is shown in Fig. 1. The proposed UWB BPF is a modification structure in [22], in which the multi-mode resonator structures are coupled to the middle ring resonator section, to achieve the required multi-notch bands. The equivalent transmission line network of the proposed filter is illustrated in Fig. 2. The interdigital coupled line is equivalent to a combination of the two signal transmission lines on two sides and a J-inverter susceptance. The multi-mode resonator coupled to the middle section of the ring resonator can be analyzed by a shunt series resonant branch, as shown in Fig. 2. Furthermore, in Fig. 1, the multi-mode resonator structure can be equivalent to an LC resonator network whose parameters are L_i and C_i with $1 \leq i \leq 5$; which are shown in Fig. 2. Therefore, each resonator can be regarded as an LC resonator, which is related to the corresponding notch band. Here, the L and C can be obtained from resonator theory.

Two capacitive-ended interdigital coupled into the I/O lines possess a wide-stop-band performance [22]. In this paper, we use the middle ring resonator to realize the multi-notch bands. The design idea and procedure of the multi-notch bands are described in Fig. 3. First, we improve the prototype filter proposed in [22] to cast a ring structure denoted as a simplified prototype filter. Then, a transition filter-1 is designed based on the simplified prototype filter by inserting a general stub into the ring resonator to produce a notch-band characteristic. As for filter-1, the inserted general stub is acted as a resonator, which is designed to provide a notch band. As a result, there is no coupling current at the output of filter-1. Therefore, the filter-1 can effectively reject the unwanted signal at corresponding frequency band. To make it suitable for dual-notch-band applications, another general stub is employed and inserted into the ring resonator based on the transition filter-1 to design a dual-notch-band filter, which is referred to as transition filter-2. The transition filter-2 can be treated as a ring resonator with two general stubs inserted into the simplified prototype filter. To render the proposed filter more useful in practice, a ring resonator with two stubs is employed to construct a tri-notch filter, referred to as transition filter-3. By considering the design procedure of the notch band filters aforementioned, an UWB band-pass filter with multi-notch bands is proposed by integrating three stubs, a ring resonator and a Stepped Impedance Resonator (SIR) into the simplified prototype filter; which is denoted as the final filter, as shown in Fig. 3. To give an insight into the performance of the proposed multi-notch-band filter, the proposed transition filters together with stubs and ring resonator are analyzed. Next, we investigate the characteristics of the single notch band to analyze the proposed transition filter-1. The geometry of the proposed transition filter-1 is illustrated in Fig. 4 and the equivalent circuits of the ring resonator are shown in Fig. 5.

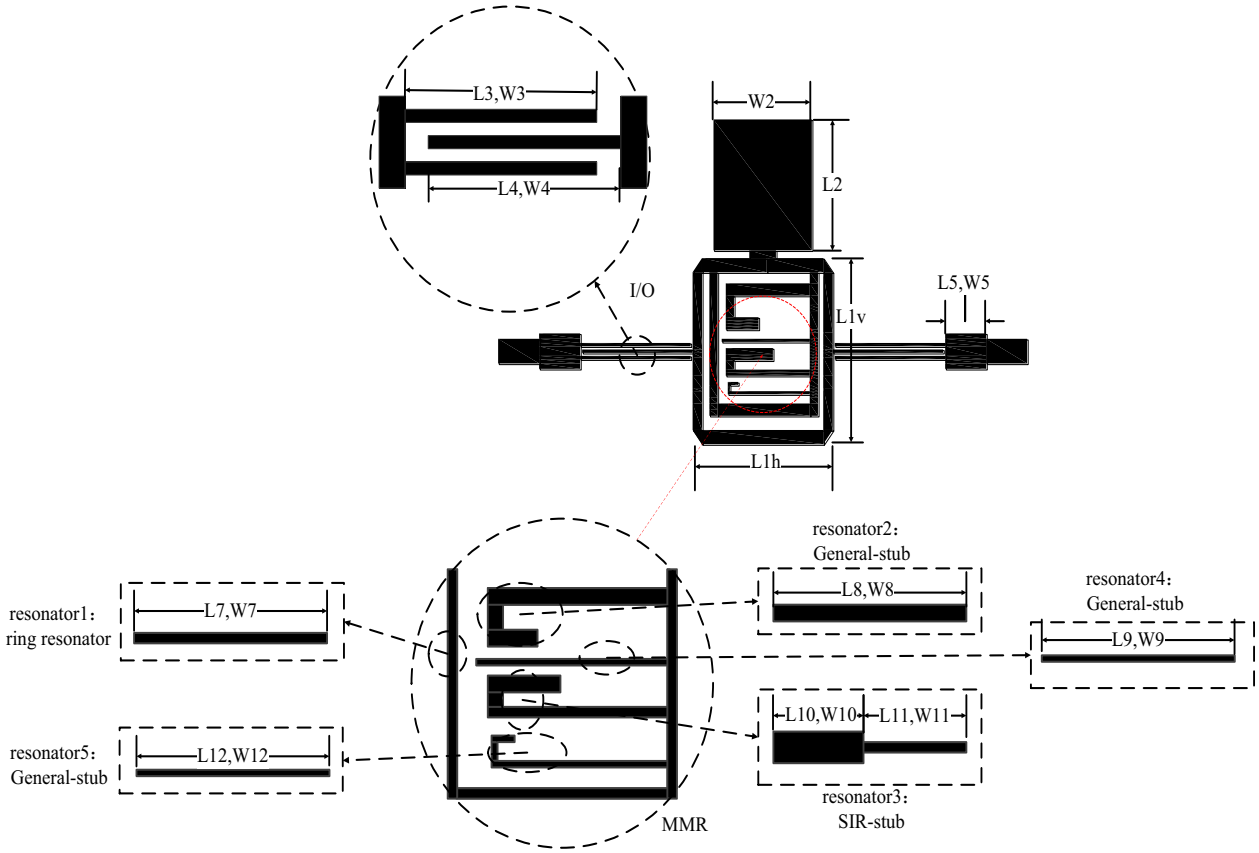

Fig. 1. Configuration and dimensions of the proposed filter.

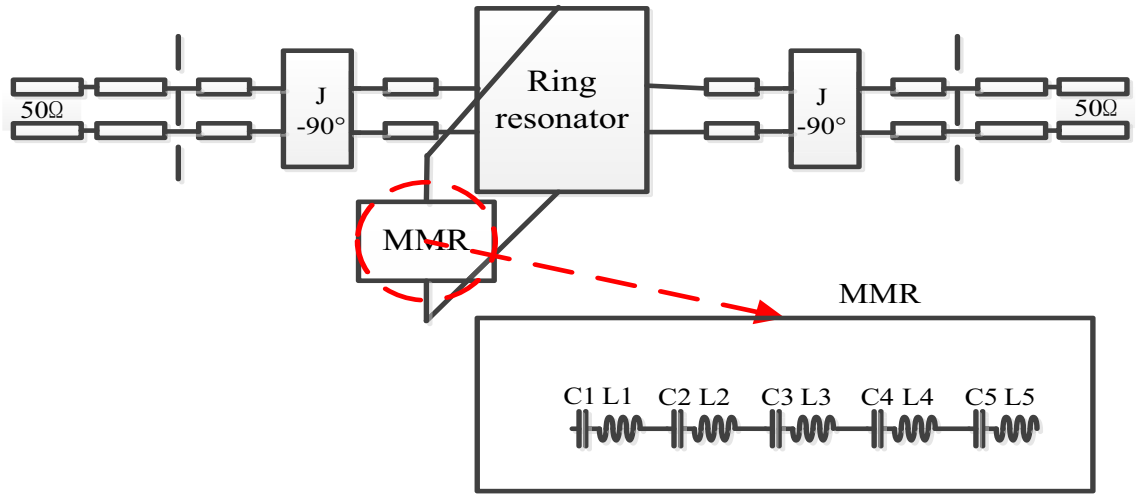

Fig. 2. Equivalent circuit network of the proposed filter.

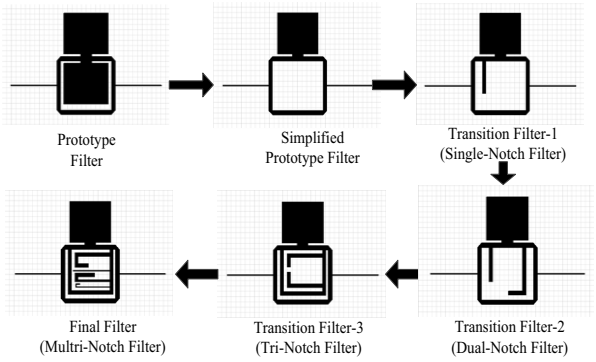

Fig. 3. Design procedure of the proposed UWB filter.

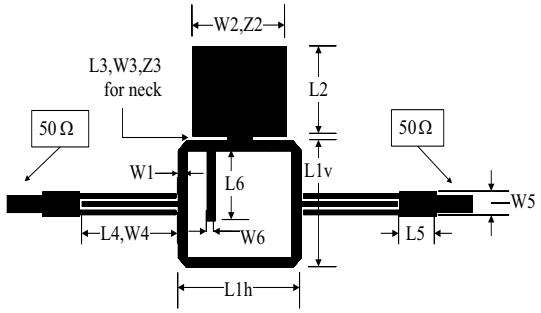

Fig. 4. Geometry of the transition filter-1.

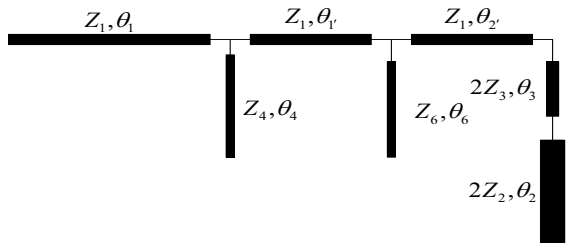

(a) Even-mode

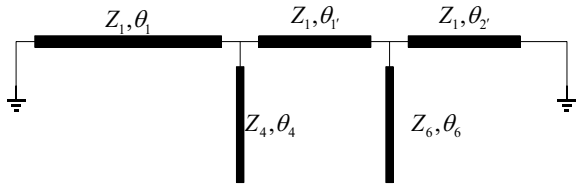

(b) Odd-mode

Fig. 5. Equivalent circuits of the ring resonator in Fig. 4.

The middle ring resonator of transition filter-1 can be analyzed based on the even and odd mode methods. Even-mode and odd-mode equivalent circuits for the ring resonator fed by the interdigital coupled lines in Fig. 4, are shown in Figs. 5 (a) and (b). On the basis of the odd-mode equivalent circuit, the odd-mode forms a pass band only, while the even-mode is designed for not only the pass-band but also the notch-band. In this paper, it is desirable to design an UWB BPF with a sharp and tunable notch-band. Thus, we will describe how to realize a notch band using the stub technique mentioned above. As the even-mode can be designed for both the pass-band and notch-band applications, we will only analyze the resonance condition about the even-mode. By considering the analysis procedure in [14, 23], the even-mode resonance condition proposed herein can be achieved and expressed by the equation below for $Y_{in}=0$. For the even-modes:

$$Y_{in}=\frac{\tan\theta_1+\left(K''\right)^{-1}\tan\theta_4+\dfrac{(\tan\theta_1'+R)}{1-\tan\theta_1'R}}{1-\tan\theta_1[(K'')^{-1}\tan\theta_4+(\dfrac{(\tan\theta_1'+R)}{1-\tan\theta_1'R})]}=0, \quad (1)$$

where,

$$R=(K''')^{-1}\tan\theta_5+\frac{\tan\theta_2'+\dfrac{1}{2}[\dfrac{(K')^{-1}\tan\theta_3+K^{-1}}{1-K'(K)^{-1}\tan\theta_3\tan\theta_2}]}{1-\dfrac{1}{2}\tan\theta_2'[\dfrac{(K')^{-1}\tan\theta_3+K^{-1}}{1-K'(K)^{-1}\tan\theta_3\tan\theta_2}]}. \quad (2)$$

In the equations above, the K, K', K'' and K''' can be expressed as:

$$K=\frac{Z_2}{Z_1}, K'=\frac{Z_3}{Z_1}, K''=\frac{Z_4}{Z_1}, K'''=\frac{Z_5}{Z_1}. \quad (3)$$

The simulation parameters are listed as follows (unit: mm): L1v=5.12, L1h=5.92, L2=4.25, L3=0.25, L4=5.39, L5=2.0, W1=0.46, W2=5.2, W3=1.3, W4=0.11 and W5=1.15. In the next step, we use these parameters to simplify the even-mode resonance condition. Based on the parameters above, we can get $\theta_6\approx 70°$ and then the length of the stub is close to $7\lambda_{notch}/36$, where λ_{notch} corresponding to the center frequency of the notch can be expressed as:

$$\lambda_{notch}=\frac{C}{f_{notch}\sqrt{\varepsilon_{eff}}}, \quad (4)$$

where, f_{notch} is the center frequency of the notch band, ε_{eff} is the effective dielectric constant and

C is the speed of light in free space. The effective dielectric constant ε_{eff} can be given using the equation (5) below:

$$\varepsilon_{eff} = \frac{\varepsilon_r + 1}{2} + \frac{\varepsilon_r - 1}{2}[(1 + 12\frac{h}{w})^{-1/2} + 0.04(1 - \frac{w}{h})^2]. \quad (5)$$

To understand the performance of the proposed transition filter-1, the transmission coefficients obtained by using IE3D are plotted in Fig. 6.

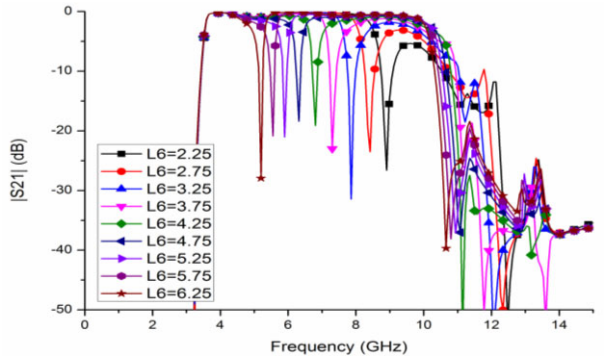

Fig. 6. Transmitted coefficient of the filter-1 for different L6 values.

Figure 6 shows the transmission characteristic of the proposed transition filter-1. The notched band moves toward the lower frequency when increasing the length of L6 and L6=4.25 mm is selected for the optimum design. In this case, we can design the notch band to use at 6.8 GHz band. To further study the nature of the performance of this filter, the current density distribution on the proposed transition filter-1at 6 GHz in the pass-band, is shown in Fig. 7, meanwhile the notch band at 6.8 GHz is obtained.

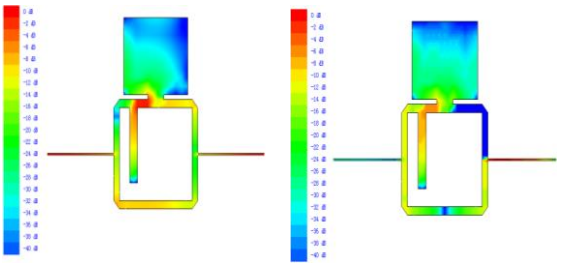

(a) 6 GHz (b) 6.8 GHz

Fig. 7. Current density distribution on the proposed transition filter-1.

It can be seen from Fig. 7, that the resonator neither resonates nor effects on the overall performance at 6 GHz in the pass-band, while the maximum current density distribution is on the stub that produces the 6.8 GHz notch band. Figure 7 (b) clearly shows that the resonator at the notched frequency is acting as a short circuit and no coupling exists on the stub at the output port. As mentioned above, the notched band can be easily controlled by adjusting the stub dimensions. In particular, the length of the stub decides the center frequency of the notch-band and the frequency bandwidth of the notch-band is determined by the stub width. Next, we will discuss the transition filter-2.

The theoretical design and synthesis of a compact UWB BPF with dual-notch-band features generated by using two inserted stubs, is shown in Fig. 8. Technically, the proposed filter design essentially exploits the open stub structures to realize dual sharp and adjustable notch-band characteristics. The corresponding lumped equivalent circuits and the equivalent circuit network of the proposed transition filter-2, are shown in Fig. 9.

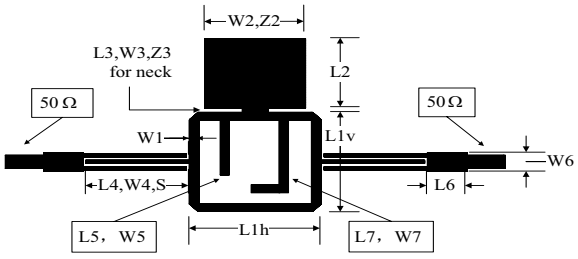

Fig. 8. Geometry of proposed transition filter-2.

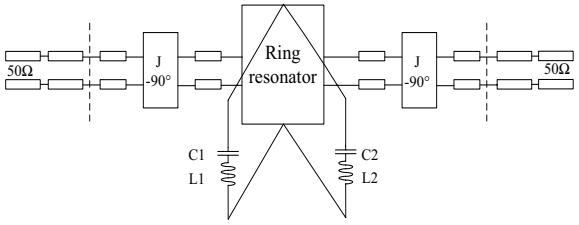

Fig. 9. Equivalent circuit network of proposed transition filter-2.

The middle ring resonator can be analyzed in terms of even and odd modes. Even-one, even-two and odd-mode equivalent circuits for the ring

resonator fed by the interdigital-coupled lines in Fig. 8, are shown in Figs. 10 (a), (b) and (c), respectively. From the odd-mode equivalent circuits, we can see that the odd-mode only designs for the pass band. On the other hand, the even-mode designs not only for the pass-band but also for the notch-band. In this paper, we design an UWB pass-band filter with two sharp and adjustable notch-bands. We only analyze the resonance condition for these even-modes and the even-mode resonance condition can be achieved for $Y_{in} = 0$.

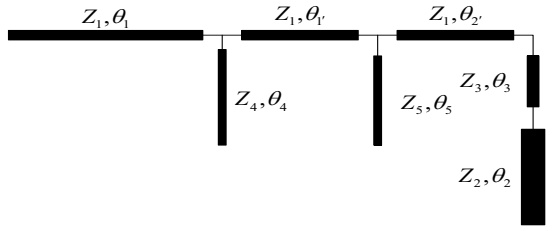

(a) Even-mode-one

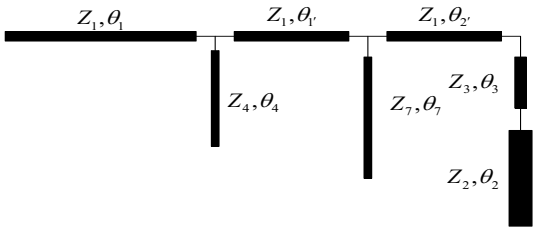

(b) Even-mode-two

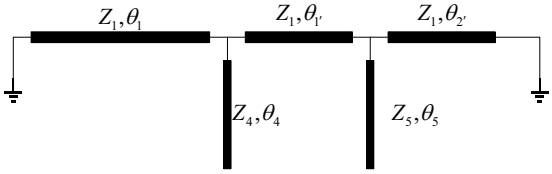

(c) Odd-mode

Fig. 10. Equivalent circuits for the ring resonator in Fig. 8; (a) even-mode one, (b) even-mode two and (c) odd mode.

The input admittance for one or two even-modes is expressed as:

$$Y_{in} = \frac{\tan\theta_1 + (K'')^{-1}\tan\theta_4 + \dfrac{(\tan\theta_1' + R)}{1-\tan\theta_1' R}}{1-\tan\theta_1[(K'')^{-1}\tan\theta_4 + (\dfrac{(\tan\theta_1' + R)}{1-\tan\theta_1' R})]} = 0, \quad (6)$$

where,

$$R = (K''')^{-1}\tan\theta_5 + \frac{\tan\theta_2' + \frac{1}{2}[\dfrac{(K')^{-1}\tan\theta_3 + K^{-1}}{1-K'(K)^{-1}\tan\theta_3\tan\theta_2}]}{1-\frac{1}{2}\tan\theta_2'[\dfrac{(K')^{-1}\tan\theta_3 + K^{-1}}{1-K'(K)^{-1}\tan\theta_3\tan\theta_2}]} \quad (7)$$

In the equation above, K, K', K'' and K''' can be expressed as:

$$K = \frac{Z_2}{Z_1}, K' = \frac{Z_3}{Z_1}, K'' = \frac{Z_4}{Z_1}, K''' = \frac{Z_5}{Z_1} \text{ or } \frac{Z_7}{Z_1}.$$

In this filter, the design parameters are listed below (unit: mm): L1v=5.12, L1h=5.92, L2=4.25, L3=0.25, L4=5.39, W1=0.46, W2=5.2, W3=1.3, W4=0.11 and W5=1.15. Next, we use these parameters to simplify the even-mode resonance condition. Based on these parameters, we can get $\theta_{5(7)} \approx 70°$ and then the length of the stub is close to $7\lambda_{notch}/36$. To understand the performance of the notch bands, the transmitted coefficients of the transition filter-2 are plotted in Fig. 11.

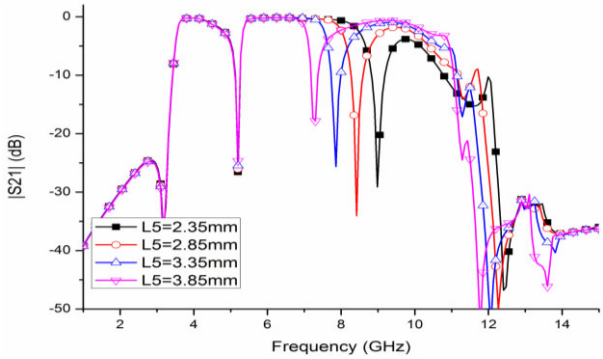

(a) Transmission coefficients with varying L5

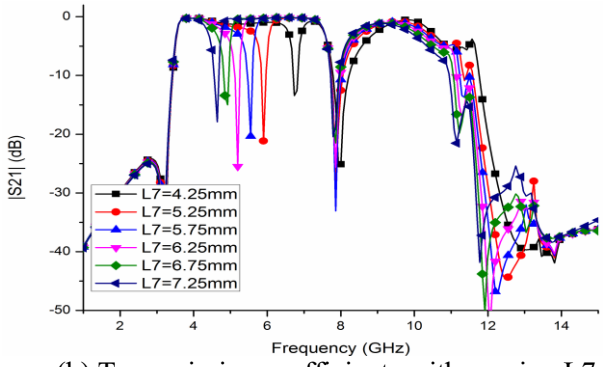

(b) Transmission coefficients with varying L7

Fig. 11. Transmitted coefficient of the transition filter-2.

Figure 11 (a) shows the transmission property of the mentioned transition filter-2 with different

L5. By increasing L5, the notched band moves toward the lower frequency. The higher notch band can be tuned from 7 GHz to 9.2 GHz. Figure 11 (b) shows the transmission property of the transition filter-2 for different L7. It is found that the notched band moves toward the lower frequency with the increment of L7 and the notch band can be tuned from 4 GHz to 7 GHz. In this paper, L5=3.35 mm and L7=6.25 mm are selected to investigate the transition filter-2. In this case, the two notch bands are located at 4.9 GHz and 7.8 GHz. To investigate the operation property of the transition filter-2, the current density distribution on the proposed middle ring resonator in both the pass-band and notch-band are illustrated in Fig. 12.

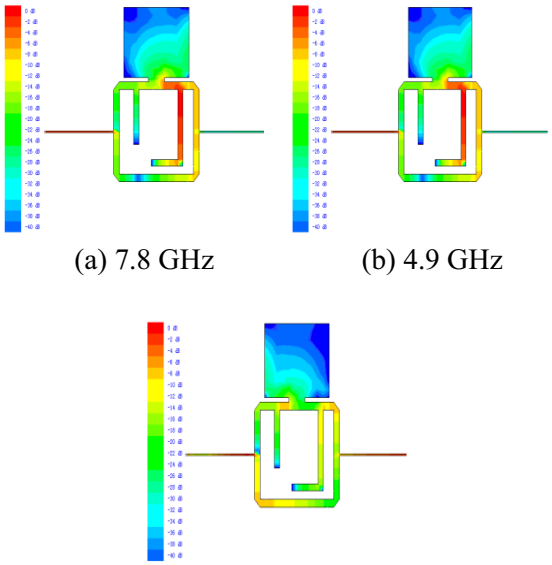

(a) 7.8 GHz (b) 4.9 GHz

(c) 6 GHz

Fig. 12. Current density distribution on the transition filter-2.

It can be seen from Fig. 12 that the current density distributions are on the transition filter-2 at 6 GHz in the pass-band. Thus, the resonator neither resonates nor affects the overall performance. At the notched frequencies 4.9 GHz and 7.8 GHz, the resonator has a focus of current density on the stubs. At the input port, the current is high while the current at the output port is low. Thus, the signal is prevented by the notch characteristics. Figures 12 (a) and (b) clearly show that the resonator at the notched frequency is acting as a short circuit and no coupling exists over the stub at the output port. As mentioned above, the frequency of the notched band can be easily controlled by adjusting the stub dimensions. In particular, the stub length decides the center frequency of the notch band and the stub width decides the bandwidth of the notch-band. For the geometry shown in Fig. 13, the proposed UWB filter with tri-notch-band characteristics, referred to as transition filter-3, is investigated in [14]. The transition filter-3 is composed of two interdigital hairpin resonator units, middle ring-stub multi-mode resonator and two 50-Ω SIR fed structures. Several folded stubs are inserted to the middle ring resonator section to achieve the tri-notch-bands.

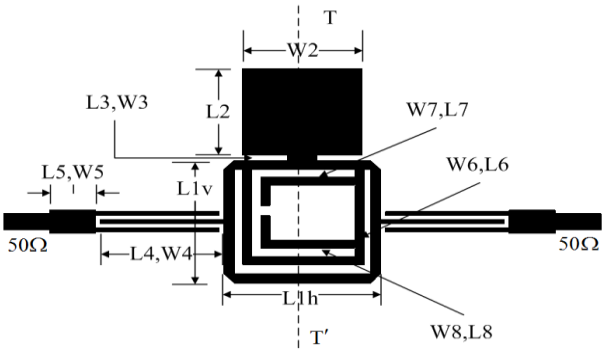

Fig. 13. Geometry of the proposed transition filter type three.

Based on the analysis and the simulated results mentioned above, an UWB filter with multi-notch-band characteristic is proposed, as shown in Fig. 1. To analyze this filter in detail, we decompose the filter to 5 resonators. Firstly, we embedded the resonator-1 and resonator-2 to the simplified prototype filter to create the dual-notch-band characteristic. The first notch-band and the second notch-band are realized by using the resonator-1 and the resonator-2, respectively. The notch characteristics of this filter are obtained by using IE3D, as shown in Fig. 14 (a). We can see from Fig. 14 (a), that with increase of the length of L8, the center frequency of the second notch band moves to the lower frequency, while the center frequency of the first notch band changes slightly. Thus, the second notch band can be tuned by adjusting the length of L8.

Secondly, the resonator-1, resonator-2 and resonator-3 are inserted into the simplified

prototype filter to create tri-notch-band characteristic. At the beginning of this design, a general stub resonator is used for designing resonator-3. The notch characteristics of this filter are shown in Fig. 14 (b). With increasing the length of L10 + L11, the center frequency of the third notch band moves to the lower frequency. In addition, the center frequency of the first notch band also shifts to the lower side. For getting a method to adjust to the third notch-band that has no effects on the first and the second notch bands, we use a Stepped Impedance Resonator (SIR) stub instead of the general stub resonator. The SIR-stub has another key parameter to adjust the notch-band. The characteristics of the SIR-stub are shown in Fig. 14 (c). With the increase of the width of W11, the center frequency of the third notch band moves to the lower frequency and the other two notch-bands remain unchanged. These three notch-bands can be effectively adjusted.

Thirdly, we insert another stub to the designed tri-notch-band filter using resonator 1, resonator 2, resonator 3 and resonator 4, to create four-notch-band characteristics. The fourth notch-band is generated by the resonator-4. The notch band characteristic is simulated by using IE3D and the simulated results are shown in Fig. 14 (d). With the increase of the length of L9, the central frequency of the fourth notch band moves towards the lower direction. At the same time, the central frequencies of the other notch bands are changed slightly. So we can control the fourth notch band by adjusting the dimension of L9.

Finally, another resonator is inserted to the four-notch-band filter to create the final filter, which is obtained by using the resonator-5. The notch characteristics of the constructed filter are simulated by using IE3D and the simulated results are shown in Fig. 14 (e). With the increase of the length of L12, the central frequency of the fifth notch band moves towards the lower frequency, while the central frequencies of the other notch bands keep nearly constant. Thus, we can control the fifth notch band by adjusting the dimension of L12. According to the analytical and the simulated results above, the designed multi-notch-band characteristics can be simultaneously obtained by choosing the proper dimensions of the middle ring-stub multi-mode resonator, the stubs and the SIR.

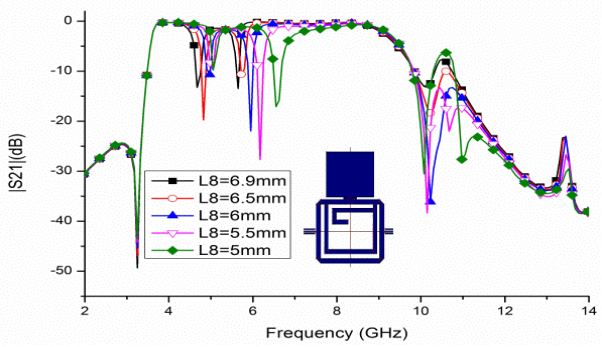

(a) L8

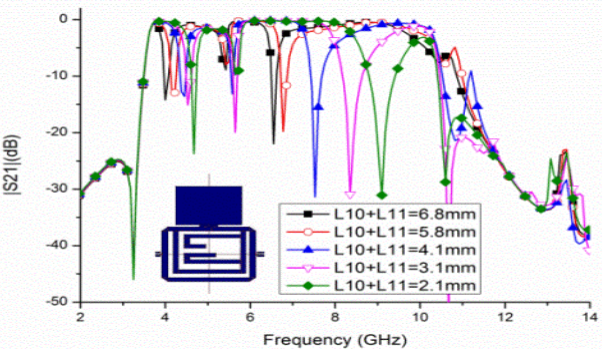

(b) L10 + L11

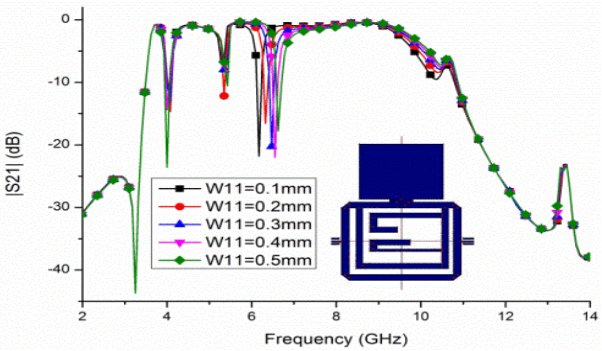

(c) W11

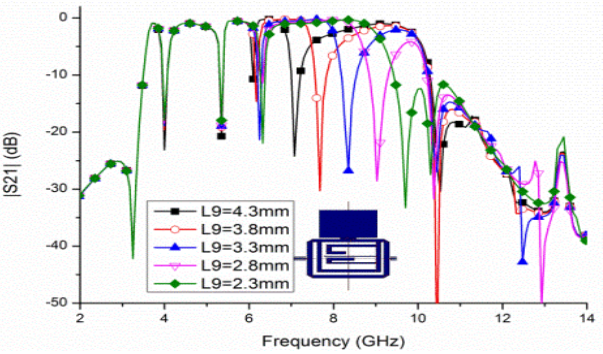

(d) L9

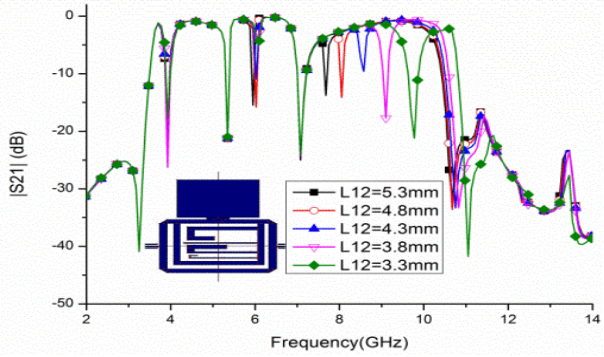

(e) L12

Fig. 14. Transmitted coefficient variation of the proposed filter.

To understand the filter property further, the current density distribution on the proposed final filter is investigated at several frequencies, as shown in Fig. 15; in which Figs. 15 (a) and (b) show the current density distribution on the multi-notch-band UWB filter at 4.5 GHz and 9 GHz in the pass-band. It can be seen that the current density distributions on the input and output port are significant, while the current density distribution on the multi-mode resonator is smaller at 4.5 GHz and 9 GHz in the pass-band; implying that the signal can be transformed from the input port to the output port in the pass-band and the multi-mode resonator has no effects on the pass band. Figures 15 (c)-(g) show the current density distributions on the proposed filter at the five notch bands. It is observed that the current density distributions on the input port are strong, while they are smaller on the output port and the current density distribution on the multi-mode resonator is very large at the notch-band frequency; implying that the signal cannot be transformed from the input port to the output port on the notch-band. These signals are rejected by the multi-mode resonator. Thus, the five notched bands can be obtained at 3.9 GHz, 5.25 GHz, 5.9 GHz, 6.8 GHz and 8 GHz. Figures 15 (h) and (i) illustrate the current density distributions on the proposed multi-notch-band UWB filter on the stop band. It can be seen that the current density distributions at 2.5 GHz and 12 GHz are mainly concentrated on the input port. The current density distributions are smaller on the multi-mode resonator in the stop-band, which means that the signals cannot be transformed from the input port to the output port in the stop-band. These signals are reflected by the interdigital coupled lines.

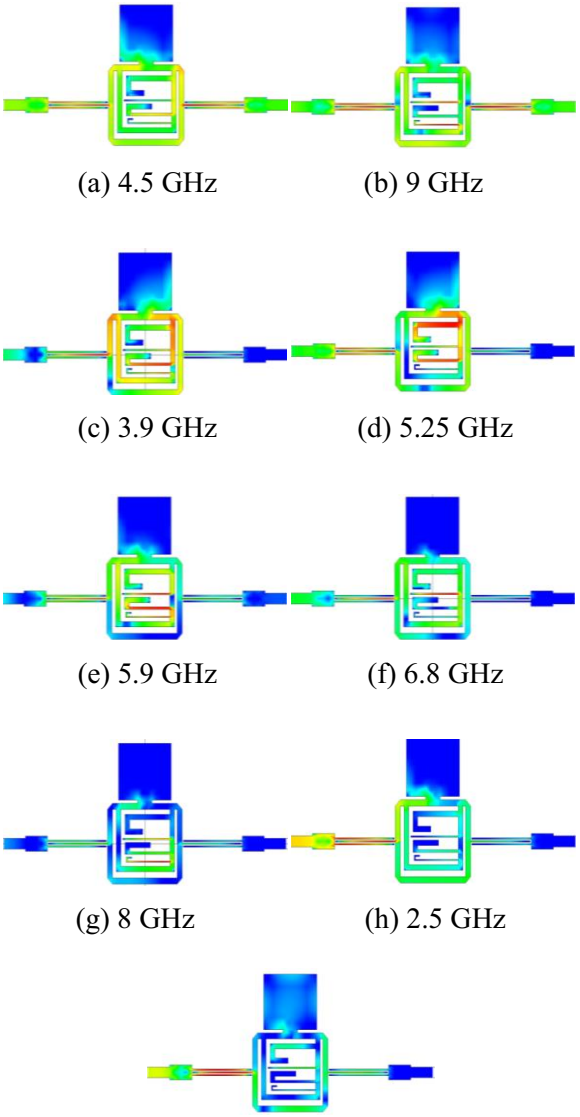

(a) 4.5 GHz (b) 9 GHz

(c) 3.9 GHz (d) 5.25 GHz

(e) 5.9 GHz (f) 6.8 GHz

(g) 8 GHz (h) 2.5 GHz

(i) 12 GHz

Fig. 15. Current density distributions on the multi-notch band UWB filter (left: input port; right: output port).

III. RESULTS AND DISCUSSIONS

To evaluate the performance of the multi-notch band UWB filter, the parameters of the designed filter are optimized numerically through IE3D. Optimal parameters of the five-notched band UWB filter are listed in Table 1. To verify the effectiveness of the proposed filter, the proposed filter is fabricated, which is shown in

Fig. 16. The filtering performance was measured by using Anristu 37347D vector network analyzer. Figure 17 demonstrates the frequency responses of the proposed filter. The measured results agree well with the simulated results. The discrepancies between the simulated and measured results may be caused by the fabrication errors.

Table 1: Dimensions of the proposed tri-notch band UWB filter

Parameter	Size (mm)	Parameter	Size (mm)
L1v	5.12	W1	0.46
L1h	5.92	W2	4.4
L2	4.25	W3	0.11
L3	5.4	W4	0.11
L4	5.4	W5	1.5
L5	2	W6	0.4
L6	0.25	W7	0.4
L7	13.8	W8	0.4
L8	6.5	W9	0.1
L9	4.3	W10	0.4
L10	1	W11	0.2
L11	3.1	W12	0.1
L12	4.8		

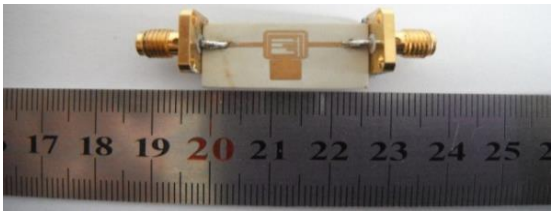

Fig. 16. Prototype of the proposed multi-notch band UWB filter.

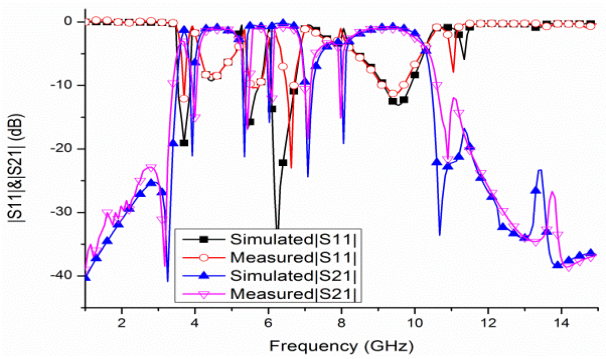

Fig. 17. Comparison between the simulated and measured results of the fabricated filter.

We can see that the fabricated filter has a measured pass-band from 3.1 GHz to 10.7 GHz with five notch bands, while the center frequencies of the notched bands are located at 3.86 GHz, 5.2 GHz, 5.9 GHz, 6.82 GHz and 7.95 GHz. The group delays shown in Fig. 18 are 0.2 ns and 0.6 ns at the six pass-bands, respectively. It is worth noting that the ring-stub multi-mode resonator can generate five notched bands at the desired frequencies with no significant influence on the wide pass-band performance. Moreover, the proposed UWB BPF has a good five-notch-band characteristic for implementing the functions of UWB radio system.

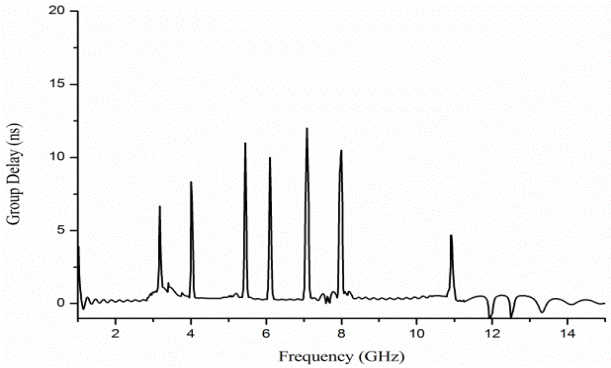

Fig. 18. Group delay of the fabricated filter.

IV. CONCLUSIONS

In this paper, a compact UWB band-pass filter with five ultra-narrow notch-band characteristic has been proposed and has been verified experimentally and numerically. The design procedures are described in details and investigated by using IE3D. By inserting a ring-stub multi-mode resonator with various stubs into an original UWB BPF, the multi-notch-band functions are obtained to reject undesired signals, such as WiMAX (3.5 GHz band), WLAN (5.2 GHz and 5.8 GHz bands), 6.8 GHz RFID and X-band (7.25 GHz to 8.0 GHz) for satellite communication applications. Simulated and measured results have demonstrated that the ring-stub multi-mode resonator can give five narrow notched bands at the undesired radio signals with no significant influence on the wide pass-band performance. The proposed filter is promising for use in UWB systems due to its simple structure, compact size and excellent performance.

ACKNOWLEDGMENT

This work was partially supported by National Defense "973" Basic Research Development Program of China (No. 6131380101). This paper is also supported by Pre-Research Fund of the 12th Five-Year Plan (No.4010403020102) and Fundamental Research Funds for the Central Universities (HEUCFT1304). The authors are also thankful to Hebei VSTE Science and Technology Co., Ltd., for providing the measuring facility.

REFERENCES

[1] "Revision of Part 15, the commission's rules regarding to ultra-wideband transmission system," *First Note and Order Federal Communication Commission, ET-Docket, FCC*, pp. 98-153, 2002.

[2] C. Hsu, F. Hsu and J. Kuo, "Microstrip bandpass filters for ultra-wideband (UWB) wireless communications," *IEEE MTT-S International Microwave Symposium Digest*, pp. 679-682, 2005.

[3] H. Wang, L. Zhu and W. Menzel, "Ultra-wideband bandpass filter with hybrid microstrip/CPW structure," *IEEE Microwave Wireless Compon. Lett.*, vol. 15, pp. 844-846, 2005.

[4] J. Huang and Q. Chu, "Compact UWB band-pass filter utilizing modified composite right/left-handed structure with cross coupling," *Progress In Electromagnetics Research*, vol. 107, pp. 179-186, 2010.

[5] H. Chen and Y. Zhang, "A novel and compact UWB band pass filter using microstrip fork-form resonators," *Progress In Electromagnetics Research*, vol. 77, pp. 273-280, 2007.

[6] L. Yang, Y. Hongchun, W. Yawei and X. Shaoqiu, "Ultra-wideband bandpass filter based on parallel-coupled microstrip lines and defected ground structure," *Applied Computational Electromagnetics Society Journal*, vol. 28, no. 1, pp. 21-26, January 2013.

[7] L. Qiang, Y. Zhao, Q. Sun, W. Zhao and B. Liu, "A compact UWB band pass filter based on complementary split-ring resonators," *Progress In Electromagnetics Research C*, vol. 11, pp. 237-243, 2009.

[8] M. Naghshvarian Jahromi and M. Tayarani, "Miniature planar UWB band pass filters with circular slots in ground," *Progress In Electromagnetics Research Letters*, vol. 3, pp. 87-93, 2008.

[9] B. Yao, Y. Zhou, Q. Cao and Y. Chen, "Compact UWB band pass filter with improved upper-stopband performance," *IEEE Microwave and wireless components Lett.*, vol. 19, pp. 27-29, 2009.

[10] H. Shaman and J. Hong, "Ultra-wideband (UWB) band pass filter with embedded band notch structures," *IEEE Microw. Wireless Compon Lett.*, vol. 17, pp. 193-195, 2007.

[11] L. Chen, Y. Shang and Y. Zhang, "Design of a UWB bandpass filter with a notched band and wide stopband," *Microwave Journal*, vol. 52, pp. 96-105, 2009.

[12] S. Gao, S. Xiao and J. L. Li, "Compact ultra-wideband (UWB) bandpass filter with dual notched bands," *Applied Computational Electromagnetics Society Journal*, vol. 27, no. 10, pp. 795-800, October 2012.

[13] C. Liu, Y. Li and J. Zhang, "A novel UWB filter with WLAN and RFID stop-band rejection characteristic using tri-stage radial loaded stub resonators," *Applied Computational Electromagnetics Society Journal*, vol. 27, no. 9, pp. 749-758, September. 2012.

[14] Y. Li, W. Li, C. Liu and Q. Ye, "A Compact UWB band-pass filter with ultra-narrow tri-notch-band characteristic," *Submitted to Applied Computational Electromagnetics Society (ACES) Journal*.

[15] C. Liu, T. Jiang and Y. Li, "A novel UWB filter with notch-band characteristic using radial-UIR/SIR loaded stub resonators," *Journal of Electromagnetic Waves and Application*, vol. 25, pp. 233-245, 2011.

[16] T. Jiang, C. Liu, Y. Li and M. Zhu, "Research on a novel microstrip UWB notch-band BPF," *Asia Pacific Microwave Conference*, pp. 261-264, 2009.

[17] P. Hsiao and R. Weng, "Compact tri-layer ultra-wideband bandpass filter with dual notch bands," *Progress In Electromagnetics Research*, vol. 106, pp. 49-60, 2010.

[18] P. Hsiao and R. Weng, "Compact open-loop UWB filter with notched band," *Progress In Electromagnetics Research Letters*, vol. 7, pp. 149-159, 2009.

[19] Y. Wu, C. Liao and X. Xiong, "A dual-wideband band pass filter based on E-shaped microstrip SIR with improved upperstop band performance," *Progress In Electromagnetics Research*, vol. 108, pp. 141-153, 2010.

[20] J. Huang, Q. Chu and C. Liu, "Compact UWB filter based on surface-coupled structure with dual notch bands," *Progress In Electromagnetics Research*, vol. 106, pp. 311-319, 2010.

[21] S. Pirani, J. Nourinia and C. Ghobadi, "Band-notched UWB BPF design using parasitic coupled line," *IEEE Microwave and wireless components Lett.*, vol. 20, pp. 444-446, 2010.

[22] C. Kim and K. Chang, "Ultra-wideband (UWB) ring resonator band-pass filter with a notched

band," *IEEE Microwave and Wireless Components Letters*, vol. 21, no. 4, pp. 206-208, 2011.

[23] C. Kim and K. Chang, "Ring resonator band pass filter with switchable bandwidth using stepped-impedance stubs," *IEEE Transactions on Microwave Theory and Techniques*, vol. 58, no. 12, pp. 3936-3944, 2010.

Yingsong Li received his B.S. degree in Electrical and Information Engineering and his M.S. degree in Electromagnetic Field and Microwave Technology from Harbin Engineering University, in 2006 and 2011, respectively. Now he is a Ph.D. candidate at Harbin Engineering University, China. He is a student member of the Chinese Institute of Electronics (CIA), IEEE and IEICE. His recent research interests are mainly in microwave theory, small antenna technologies and computational electromagnetic.

Wenxing Li received his B.S. and M.S. degrees from Harbin Engineering University, Harbin, Heilongjiang, China in 1982 and 1985, respectively. He is currently a full professor at College of Information and Communication Engineering, Harbin Engineering University, China. He is also the head of Research Centre of EM Engineering & RF Technology. He visited the Department of Electrical Engineering of the Pennsylvania State University, USA from June to August, 2010. He also visited the Oriental Institute of Technology, Taiwan from August to October, 2010. He is also the organizer of the 30th Progress in Electromagnetics Research Symposium (PIERS), the IEEE International Workshop on Electromagnetics (iWEM), the TPC of 2012 Asia-Pacific Symposium on Electromagnetic Compatibility (APEMC 2012) and the 2012 Global Symposium on Millimeter Waves (GSMM 2012). His recent research interests are mainly in computational electromagnetic, microwave engineering, modern antenna design and microwave and millimeter wave circuits.

Chengyuan Liu received his B.S. degree in Electrical and Information Engineering and his M.S. degree in Electromagnetic Field and Microwave Technology from Harbin Engineering University, 2006 and 2011, respectively. Now he is a Ph.D. candidate at Harbin Engineering University, China. He serves as receivers for the Journal of Electromagnetic Waves and Applications, Journal of Microwaves, Optoelectronics and Electromagnetic Applications, Progress in Electromagnetics Research Series and Journal of Electromagnetic Waves and Applications. His research interests are mainly in microwave theory, UWB antenna and UWB filters.

Wenhua Yu joined the Department of Electrical Engineering of the Pennsylvania State University and has been a Group Leader of the electromagnetic communication lab since 1996. He received his Ph.D. in Electrical Engineering from the Southwest Jiaotong University in 1994. He worked at Beijing Institute of Technology as a Postdoctoral Research Associate from February 1995 to August 1996. He has published one book on CFDTD software and two FDTD books: Conformal Finite-Difference Time-Domain Maxwell's Equations Solver: Software and User's Guide (Artech House, 2003), Parallel Finite-Difference Time-Domain (CUC Press of China, 2005, in Chinese) and Parallel Finite-Difference Time-Domain Method (Artech House, 2006). He has published over 100 technical papers and four book chapters. He developed and created the Computer and Communication Unlimited Company (http://www.2comu.com) and serves as its President. He is a Senior Member of the IEEE. He was included in Who's Who in America, Who's Who in Science and Engineering, and Who's Who in Education. He is also a visiting professor and Ph.D. Advisor of the Communication University of China. Yu's research interests include computational electromagnetic, numerical techniques, parallel computational techniques and the theory and design of parallel computing systems.